

VALENCE ELECTRON DISTRIBUTIONS IN TRANSITION METAL COMPLEXES:  
STATE OF THE ART STUDIES

Ronald Mason and Joseph N. Varghese

School of Molecular Sciences, University of Sussex, Brighton BN1 9QJ, U.K.

ABSTRACT

A study of valence electron density distributions in transition metal complexes is described using the novel method of polarised neutron diffraction.

INTRODUCTION

Some thirty years of researches have taken discussions of bonding in transition metal complexes from the simple crystal field theories - with their early useful rationalisation of some magnetic, spectral and associated properties of complexes - through semi-empirical models and, finally, to ab-initio molecular orbital theories; the early success of the valence bond theory has not been followed up, largely on account of computational convenience. Running through all of this is the recognition that the redistribution of the valence electrons on bond formation, on which chemistry is based, can be assessed only by indirect evidence. Experimental studies of bonding have nearly always related to molecular energy levels, it being relatively rare that direct conclusions can be drawn on the spatial relationships of electrons in bonds. Spectroscopic experiments provide, albeit with certain assumptions, molecular eigenvalues; only diffraction experiments provide a direct link between observations (reflexion intensities) and molecular eigenfunctions.

The history of the application of X-ray diffraction to studies of electron densities in crystals goes back many years - sodium chloride and diamond featured early. Dawson's work on diamond (Ref.1) was particularly noteworthy for it showed, for the first time, how 'forbidden' X-ray intensities could be explained on the basis of aspherical electron densities at each carbon atom. Even in 1960, two dimensional X-ray photography with visually estimated intensities could demonstrate, in addition to hydrogen atoms, nitrogen lone pair features in a largish organic molecule (Ref.2) (Fig.1). In the 1970's we have seen improvements in data

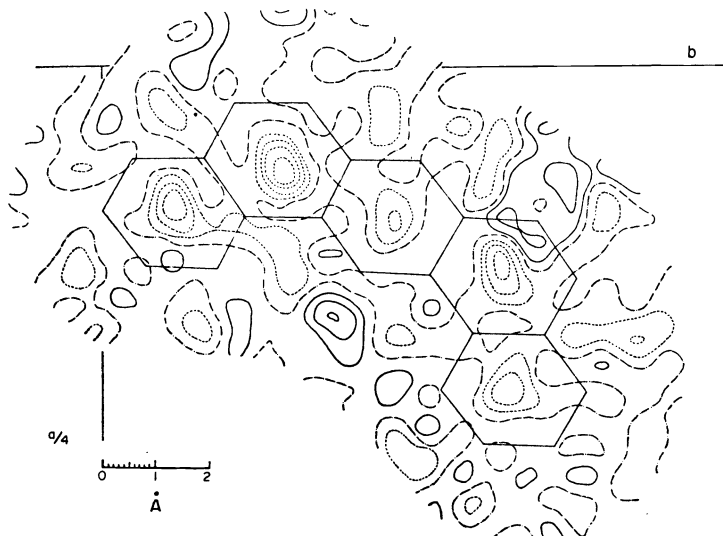


Fig.1. The electron density of 1,2:8,9-dibenzacridine from which all atoms have been subtracted (Ref.2).

accuracy and, coupled with conventional neutron scattering experiments, a number of reports (Ref.3) have described the distribution of electrons in small molecules containing elements from the first row of the Periodic Table. When we move on to complexes of transition metal

ions, the X-ray experiments begin to have the rather obvious limitations associated with the significant determination of small electronic redistribution in the presence of the high local densities associated with the metal ions. Even so a significant corpus of observations is to hand (Ref.4) which, *inter alia*, have demonstrated aspherical electron densities around the metal atoms in simple complexes and the lack of significant density between the metal atoms in molecules where for a variety of reasons (18-electron accountancy; metal to metal separation and so on) one infers direct metal to metal bonding. The status of the X-ray method is being reviewed by P.Coppens at this Conference (Ref.5) and so little more needs saying here. Rather we shall focus on the exploration of what has been one of the most significant physical properties of transition metal complexes: paramagnetism; and the determination of some eigenfunctions of open shell molecules using the very novel method of polarised neutron scattering.

#### The experiment

The polarised neutron technique provides an extremely sensitive method for studying magnetisation distributions in crystalline materials. A neutron interacts with atomic nuclei through the strong nuclear interaction and with electrons by virtue of its magnetic moment. The magnetisation density in a crystal is due both to the intrinsic magnetic moment of electrons (spin) and to the magnetic moment generated by moving electrons (orbital magnetisation). The magnetisation density due to spin reflects the spatial distribution of the unpaired electrons, but that due to their orbiting motion is less simply interpreted.

An instrument for doing polarised neutron diffraction experiments is illustrated in Fig.2.

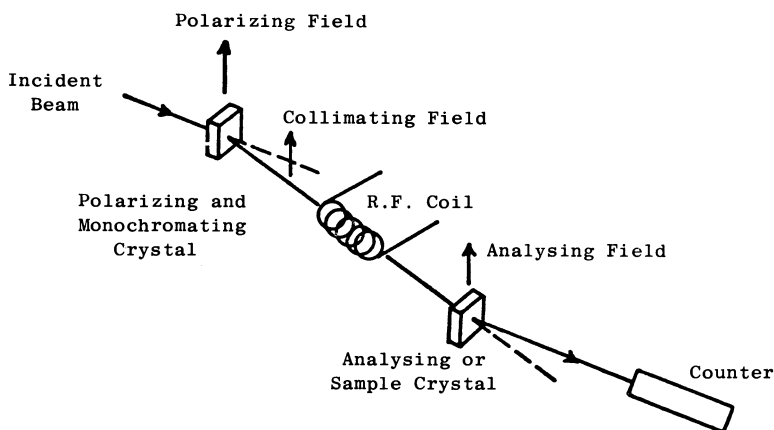


Fig.2. A schematic layout of a polarised neutron diffraction experiment.

A monochromatic polarised neutron beam is produced by Bragg reflection of polychromatic unpolarised neutrons from the reactor by a polarising crystal. At some point in the flight path to the specimen a 'spin flipper' is introduced: an RF coil (tuned to the Larmor frequency) or one of a number of other devices. The experiment, then, is to determine a 'flipping ratio' for each Bragg reflection, that being the numerical ratio of counting rates for the 'up' and 'down' polarisation states of the neutrons incident upon the specimen. In the case of a centrosymmetric crystal, the flipping ratio  $R$  is

$$R = \frac{N^2 + M^2 + 2NM}{N^2 + M^2 - 2NM} = \left( \frac{1 + \gamma}{1 - \gamma} \right)^2 \quad \text{where } \gamma = \frac{M}{N}$$

here  $M$  and  $N$  are the magnetic and nuclear structure factors of a given Bragg reflection;  $N$  is determined by a normal (unpolarised) neutron scattering experiment. When magnetic neutron scattering is much weaker than nuclear scattering we have

$$R = 1 + 4\gamma$$

#### Derivation of spin densities

Early use of magnetic structure factors was confined to detailed studies of the form (scattering) factors of simple systems such as the metals iron, cobalt and nickel (Ref.6). With increasing sophistication of equipment, increasing neutron fluxes and a developing formalism for calculating magnetic structure factors, the study of more complex magnetic systems having chemical interest has become possible.

We need then to set down some relevant approaches and the theoretical models that allow them to be developed. We noted earlier that the magnetisation density in a crystal reflects spin and orbital contributions. Where, as in some of the examples we discuss below, we have complex ions with orbitally non-degenerate ground states, we can associate the magnetisation density largely with the appropriate 1-electron spin density functions. The spin distribution may be expressed in terms of the partial occupation of molecular orbitals, accompanied by some polarisation of fully occupied orbitals.

Quite the simplest utilisation of the Bragg magnetic structure factors is to produce their Fourier transform. Two illustrations of this procedure are shown in Figs. 3 and 4. Figure 3 is the Fourier series which gives the magnetisation density in the  $\text{CrF}_6^{3-}$  ion in crystals of  $\text{K}_2\text{NaCrF}_6$  (Ref.7); Fig.4 is the corresponding (two dimensional) density in a copper(II) dimer (Ref.8). But the limitations attached to quantitative interpretations of Fourier

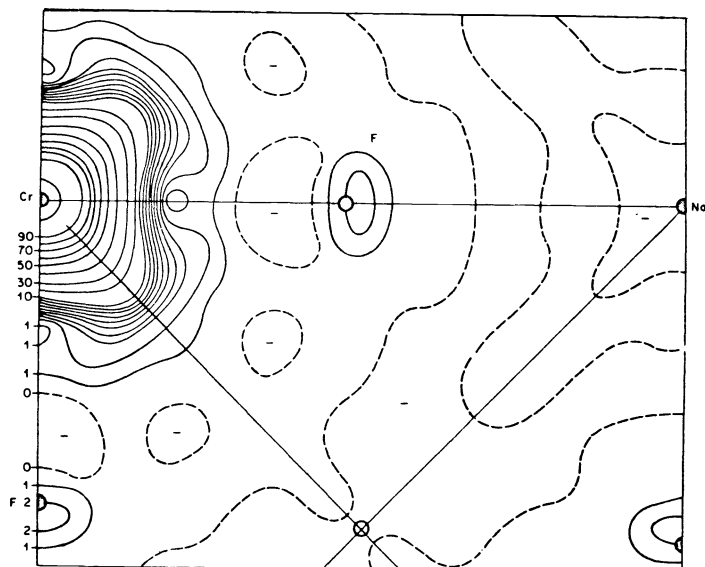


Fig.3. Fourier section through the Cr and F sites obtained from magnetic data on  $\text{K}_2\text{NaCrF}_6$  (Ref.7).

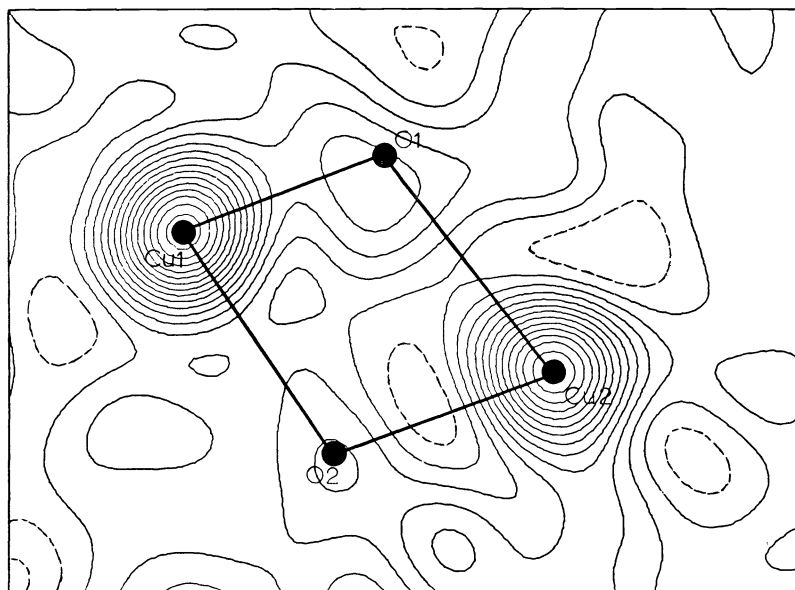


Fig.4. Fourier projection on the a b plane obtained from magnetic scattering data of aquabis(bipyridyl)di- $\mu$ -hydroxo-sulphato dicopper(II) (Ref.8).

series are well-known - they are, for the most part, concerned with series termination effects. In conventional crystallography, quantitative data can be obtained by Difference Fourier methods or least squares methods; we emphasise the second approach.

The magnetic structure factor is readily expressed as

$$M(\underline{k}) = \sum_n f_n(\underline{k}) M_n \exp\{i \underline{k} \cdot \underline{r}_n\}$$

with  $f(\underline{k})$  a magnetic form factor for a given atom,  $n$ , being

$$f(\underline{k}) = \frac{\int m(\underline{r}) \exp(i \underline{k} \cdot \underline{r}) d\tau^3}{\int m(\underline{r}) d\tau^3}$$

$m(\underline{r})$  is the atom's magnetisation density.  $M_n$  is the magnetic moment of the  $n^{\text{th}}$  atom positioned at  $\underline{r}_n$  from the origin. The summation is over all atoms. When the magnetisation is due to electrons in a single unfilled shell, the form factor becomes

$$f(\underline{k}) = \sum_l A_l(\underline{k}) \langle j_l(l|\underline{k}|) \rangle$$

where

$$\langle j_l(\underline{k}) \rangle = \int_0^\infty U^2(r) j_l(kr) r^2 dr$$

$j_l(kr)$  is the spherical Bessel function of order  $l$  and  $U^2(r)$  the radial distribution function of electrons in the open shell. The  $A_l(\underline{k})$  are coefficients which depend on the scattering vector  $\underline{k}$  and on the magnetic configuration. In general, 'd' electrons have three coefficients  $A_0$ ,  $A_2$  and  $A_4$  which are non-zero;  $A_0$  is a coefficient which reflects spherical symmetry while  $A_2$  and  $A_4$  contain, as it were, quantisation of spin and 'directionality' of bonding. When orbital contributions are present, they are often estimated via a dipole approximation (Ref.9)

$$f(\underline{k}) = 2S \langle j_0(\underline{k}) \rangle + L (\langle j_0(\underline{k}) \rangle + \langle j_2(\underline{k}) \rangle)$$

We showed, in an early note (Ref.10), how polarised neutron scattering data could define non-spherical d- and p-electron distributions: for the  $(\text{CrF}_6)^{3-}$  ion a configuration of  $t_{2g}^{2.61(2)}$  was defined with delocalisation of 0.11(3)e on to each fluorine atom; for  $\text{COCl}_4^{2-}$ , Figgis, Reynolds and Williams (Ref.11) have similarly modelled the spin density with a determination of the cobalt 3d orbital population as  $t_2^{2.71(15)}$  e  $0.0 \pm 0.1$  spins and the spin population in each chlorine being mainly in the p  $\sigma$  orbital ( $0.06 \pm 0.01$  spins). This early approach had definitional value - it indicated the intrinsic sensitivity of the magnetic scattering data to non-spherical features of the metal's spin density and to covalence parameters. We now describe (Ref.12,13) a more general way of presenting results and, in particular, of making comparisons with, say, ab initio molecular orbital calculations of spin densities.

Whether we have X-ray, neutron-nuclear or neutron-spin scattering, the generalised structure factor can be written

$$F(\underline{k}) = \sum_{\text{cell}} f_j(\underline{k}) \exp\{-i 2\pi \underline{h} \cdot \underline{x}_j - \underline{h}^T \underline{\beta}_j \underline{h}\}$$

where  $\underline{h} = 2\pi (h a^* + k b^* + l c^*)$

$\underline{h} = (h, k, l)$  are the Miller indices with respect to the reciprocal lattice cell edges  $a^*$ ,  $b^*$ ,  $c^*$ ; the run extends over all centres  $j$  in the unit cell;  $\underline{x}_j$  and  $\underline{\beta}_j$  are the positional coordinates and the mean squares displacement tensor of the centre  $j$ .

The scattering (form) factor  $f_j$  associated with the centre  $j$  is given by the one centre density representation as

$$f_j(\underline{k}) = \int \rho_j(r, \theta, \phi) \exp(i \underline{k} \cdot \underline{r}) d\tau = f_j(S, \alpha, \beta)$$

$\rho_j$  is the one centre electron (magnetisation) density associated with the centre  $j$ ;  $\rho_j(r, \theta, \phi)$  and  $(S, \alpha, \beta)$  are the components of  $\underline{r}$  and  $\underline{k}$  in spherical polar coordinates with respect to a local orthogonic frame of reference on the centre  $j$ .

In a multipole expansion (Ref.12) the density is expanded as a linear sum of density fragments

$$\rho_{\ell m}(r, \theta, \phi) = M_{\ell}^m N_{\ell}^m Z_{\ell}^m(\theta, \phi) R(r)$$

$$\ell = 0, 1, 2, 3, 4, \dots$$

$$-\ell \leq m \leq \ell$$

$R(r)$  is the radial density distribution describing the density around the centre  $j$ ,  $Z_{\ell}^m$  are multipole functions (Surface or Tesseral Harmonics) given by

$$Z_{\ell}^m(\theta, \phi) = Y_{\ell}^{|m|}(\cos \theta) \cos(|m|\phi) \quad m \geq 0$$

$$= Y_{\ell}^{|m|}(\cos \theta) \sin(|m|\phi) \quad m < 0$$

$Y_{\ell}^m$  are associated Legendre functions and  $N_{\ell}^m$  a normalisation factor which requires

$$\int |\rho_{\ell m}| d\tau = 2$$

$M_{\ell}^m$  is the population of the multipole fragment  $\rho_{\ell m}$  and is normalised so that it becomes a measure of the number of electrons transferred from the negative to positive lobes of the surface harmonic (Ref.14).

Fourier transforms of multipole density fragments are

$$f_{\ell m}(S, \alpha, \beta) = \int \rho_{\ell m}(r, \theta, \phi) \exp(-i \mathbf{k} \cdot \mathbf{r}) d\tau$$

$$= i^{\ell} M_{\ell}^m N_{\ell}^m 4\pi \langle j_{\ell}(Sr) \rangle Z_{\ell}^m(\alpha, \beta)$$

where  $\langle j_{\ell}(Sr) \rangle = \int_0^{\infty} R(r) j_{\ell}(Sr) r^2 dr$

and  $S = |\mathbf{k}| = 4\pi \sin \theta \lambda^{-1}$

and  $j_{\ell}$  are spherical Bessel functions.

Thus the structure factor can be recast in multipole terms as

$$F(\mathbf{k}) = \sum_{\substack{\text{Cell} \\ \text{centres } n}} \left\{ \sum_{\ell=0}^{\infty} \sum_{m=-\ell}^{\ell} i^{\ell} M_{n,\ell}^m N_{\ell}^m 4\pi \langle j_{n,\ell} \rangle Z_{\ell}^m(\alpha, \beta) \cdot \exp(-i 2\pi \mathbf{h} \cdot \mathbf{x}_n - \mathbf{h}^T \cdot \mathbf{\beta}_n \cdot \mathbf{h}) \right\}$$

For the most part, this expression is adequate if terms up to hexadecupoles are included. There are often times when the number of non-zero multipoles is determined by local (crystallographic) symmetry arguments. A least squares convergence of the set of  $F(S)$  to the observed structure factors is via the optimisation of  $M_{n,\ell}^m$ , the  $\mathbf{x}_n$  and  $\mathbf{\beta}_n$  having been established by a conventional neutron scattering experiment. The radial function  $R(r)$  is constructed from Hartree-Fock or, perhaps, simple Slater functions; flexibility can be achieved via Kappa refinement methods (Ref.15) or by a Taylor expansion technique (Ref.16).

We have shown (Ref.17) how it is possible to interpret multipole populations in terms of chemical 'orbital' populations: by a simple linear transformation 'orbital' populations determined from one-centred orbital scattering factors are constrained multipole refinements - for 'd' orbitals up to hexadecupole level and for 'p' orbitals up to the quadrupole level. In determining 'orbital' populations one must remember that two centre orbital product terms are projected into one-centre terms, so any one-centre density representation will have built into it the projected two-centre density functions. 'Orbital' populations obtained by single centre density functions are related to the diagonal elements of the Dirac density matrix and should reflect the spin state of the metal ion.

But we believe a more valuable interpretation of multipole parametrisations of the spin density comes from a reconstruction of the total spin density from the multipole density fragments via the equation (Ref.12,13)

$$\rho(r) = \sum_{\text{Sphere centres } j} \sum_{l, m} \rho_{lm}^i(r, \theta, \phi)$$

where the sum is over a sphere which contributes to the density of the cluster.

### The results

Our first example of the quality of information that can be obtained from experiment and the correlation with theories of open shell molecules is summarised, in effect, by Fig.5. The experimental spin density (Fig.5a) shows typical 'd' orbital spin density around the chromium ion, a transfer of spin density to a fluorine  $2p\pi$  orbital and a negative spin density in the Cr - F  $\sigma$ - antibonding orbital. The transformation (Ref.17) of the multipole populations into 'local orbital' populations demonstrated a  $t_{2g}^{2.76(1)}$  configuration on the metal, no significant population in the 'e' orbitals, and a spin density of 0.31(0) in a metal 4s orbital; there is a spin transfer to the fluorine ligands which effectively includes a redistribution of 0.02e from the  $\sigma$ - to the  $\pi$ - bond framework with a negative  $p_z(P(\sigma))$  orbital population of 0.05e (and a consequent +0.03e in the  $2p\pi(x,y)$  orbitals). Spin polarised Hartree-Fock calculations give the spin transfer coefficients for Cr(III) in  $\text{CrF}_6^{3-}$  as -0.022e and +0.026e for  $f\sigma^*$  and  $f\pi$  (semi-empirical molecular orbital) (Ref.19) and -0.048e and +0.010e from an X- $\alpha$  calculation (Ref.20). More conveniently Figs. 5b and 5c summarise our calculations, at a double zeta level, based on restricted and

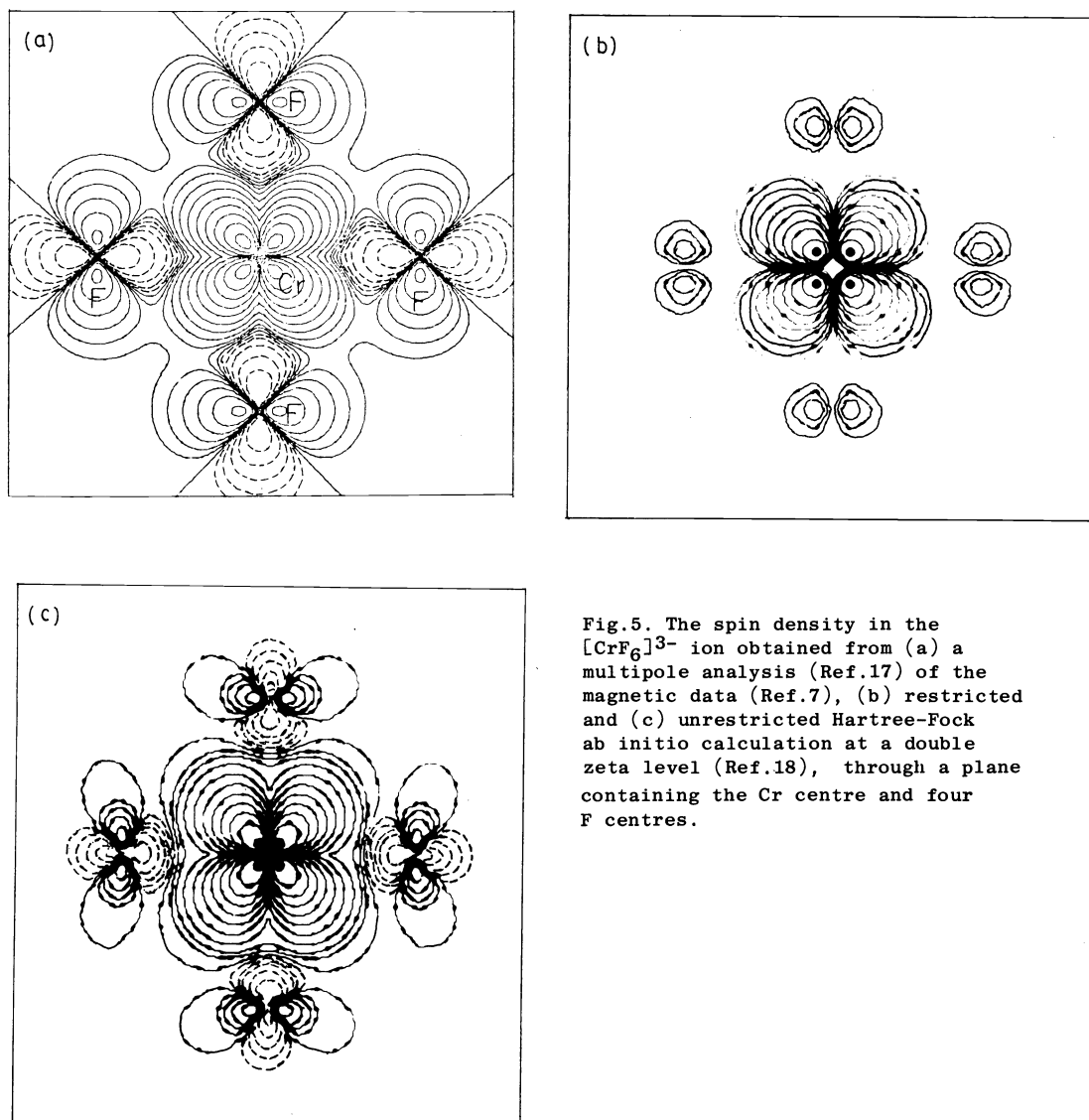


Fig.5. The spin density in the  $[\text{CrF}_6]^{3-}$  ion obtained from (a) a multipole analysis (Ref.17) of the magnetic data (Ref.7), (b) restricted and (c) unrestricted Hartree-Fock ab initio calculation at a double zeta level (Ref.18), through a plane containing the Cr centre and four F centres.

unrestricted Hartree-Fock theories; the comparison shows the importance of unrestricted Hartree-Fock in representing adequately the exchange correlation effects ( $\rho^\sigma$  versus  $\rho^\pi$ ) which are so evident from experiment. (It is worth noting here that the calculated wave-functions are a much more sensitive test of theory than the corresponding eigenvalues.)

Next we look at the spin density in the  $\text{CoCl}_4^{2-}$  determined from the multipole analysis (Ref.21) of magnetic and structure factors (Ref.22) provided by diffraction from magnetically polarised crystals of  $\text{Cs}_3\text{CoCl}_5$ . Figure 6 shows 'mouse ears' of spin density centred

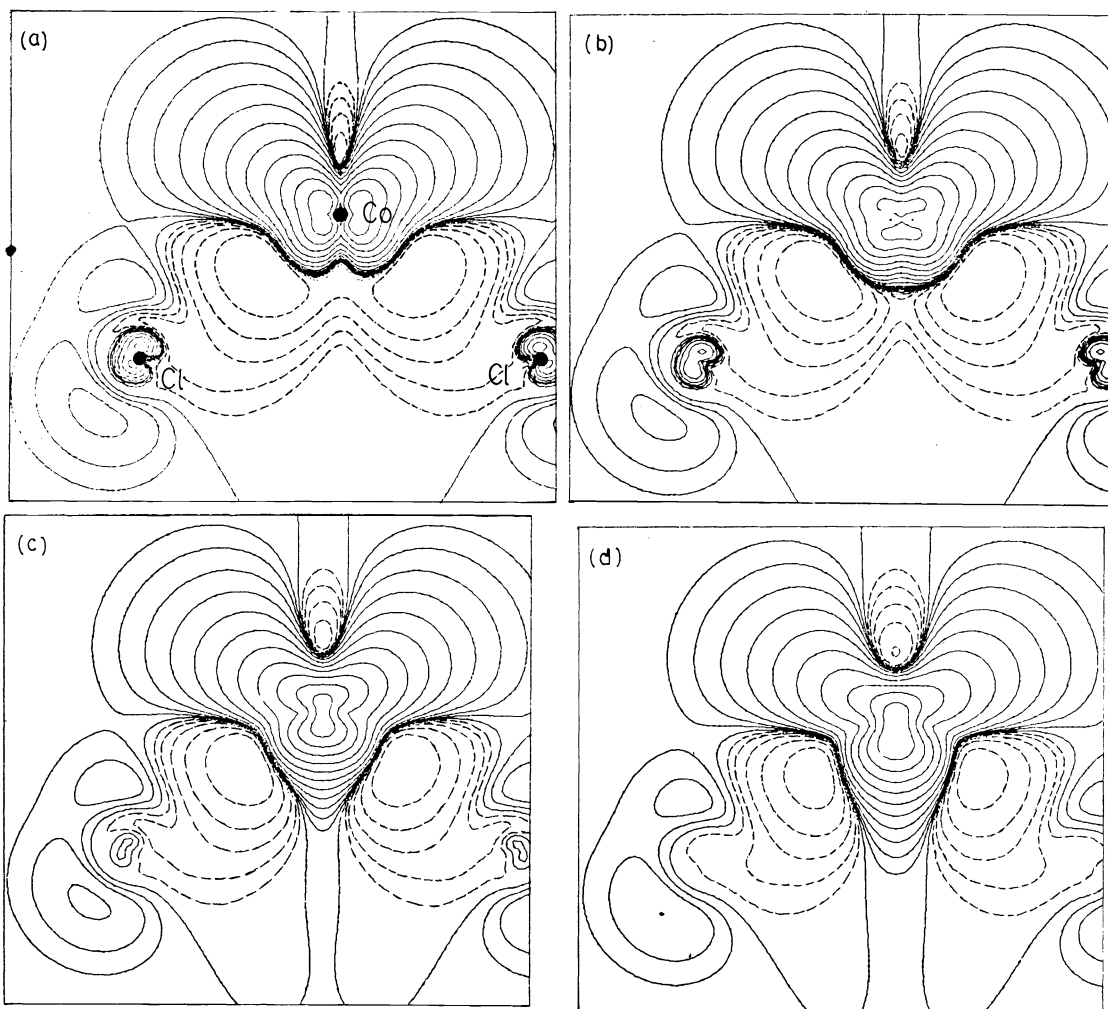


Fig.6. The spin density in the  $(\text{CoCl}_4)^{2-}$  ion in  $\text{Cs}_3\text{CoCl}_5$  obtained from a multipole analysis (Ref.21) of magnetic data (Ref.22) for (a) in the plane parallel to the c-axis of Co and two chlorine, (b) at  $0.2\text{\AA}$ , (c)  $0.4\text{\AA}$ , (d)  $0.6\text{\AA}$  above the plane.

at the cobalt, a sharp concentration of density at the chlorine centres and, once more, a significant negative spin density in the metal-ligand  $\sigma$ -framework. The succeeding maps show the spin densities in sections of  $0.2\text{\AA}$ ,  $0.4\text{\AA}$  etc. above the plane containing the Cl - Co - Cl nuclei and show the emergence of the  $\sigma$ -antibonding state with its positive spin density directed away from the ligand and the negative spin density directed towards the chlorines. The orbital populations determined by appropriate transformation of the multipole population parameters are

$$d_{xy} \quad 0.88(8) \quad d_{xz,yz} \quad 0.87(7) \quad d_{x^2-y^2} \quad 0.16(8) \quad d_{z^2} \quad -0.02(6)$$

in other words, essentially  $t_2^{2.62(7)} e^{0.14(7)}$

with the chlorine calculating at

$$p_x \quad -0.01(2), \quad p_y \quad 0.03(2), \quad p_z \quad 0.06(1)$$

There is no significant population of the metal 'e' orbitals although a population of  $d_{x^2-y^2}$  would be consistent with the deviation from Td symmetry;  $\sigma$ -bonding is significant;  $\pi$ -bonding is at least three times less so. We shall compare the experimental (Ref.21) and theoretical spin densities in detail elsewhere (Ref.18).

So much then for the quantitative information that we can now obtain experimentally on the eigenfunctions of open-shell molecules and the quality of theories that are needed to match these data. But we can add that while we have chosen, for obvious reasons, to look at 'natural' paramagnetic molecules (and hence at only, at best, non-bonding spin density distributions) we can anticipate the move towards studies of cationic species and hence of the orbital character of bonding states. An examination of multiple bond orders between metals would be of high interest and feasibility studies of bond orders of 3.5 has begun. (Ref. 25).

The most complex system we have studied, and it illustrates a different emphasis of application of polarised neutron scattering, is aquabis(bipyridyl)di- $\mu$ -hydroxo-sulphato di-copper(II) (Ref.8, 23). Figure 6 shows the spin densities corresponding to the experimentally determined multipoles: in (a) only the scalar, dipoles, quadrupoles, octupoles and hexadecupoles on the copper atoms and scalar moments on the oxygenations were refined in the least squares analysis; in (b) two dipole moments on the oxygen atoms were added to the analysis; in (c) two quadrupole moments were added to the scalar and dipole moments being refined on the bridging ligands.

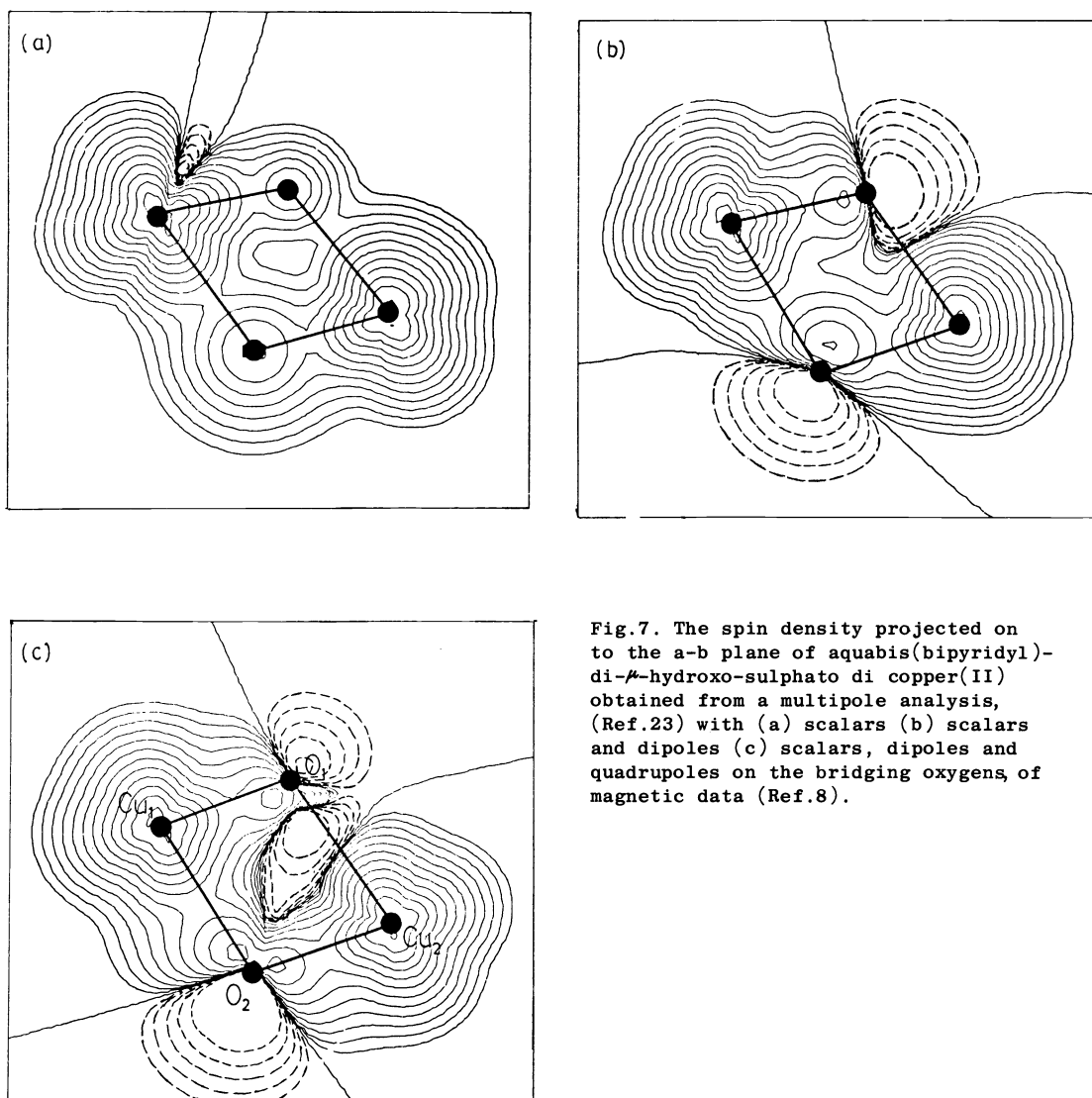
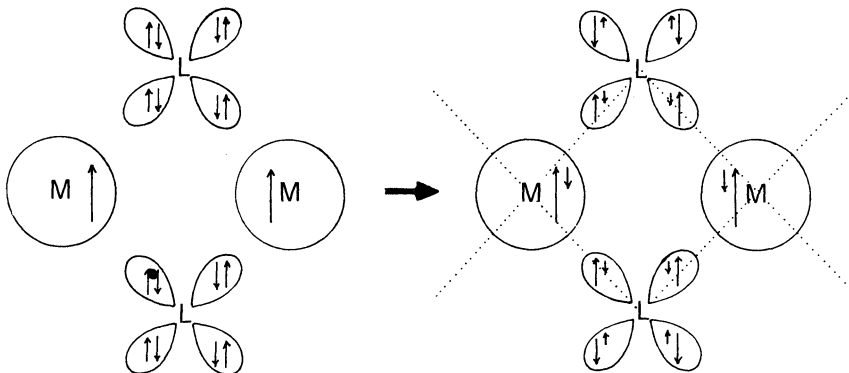


Fig.7. The spin density projected on to the a-b plane of aquabis(bipyridyl)-di- $\mu$ -hydroxo-sulphato di copper(II) obtained from a multipole analysis, (Ref.23) with (a) scalars (b) scalars and dipoles (c) scalars, dipoles and quadrupoles on the bridging oxygens, of magnetic data (Ref.8).



Figures 7a - 7c show essential invariance and equivalences of the spin densities in the  $d_{x^2-y^2}$  orbitals of the copper ions while the similar features of the oxygen spin densities in Figs. 7b and 7c indicate that inclusions of higher multipoles on the oxygen atoms is unnecessary. Quantitatively, the experimental spin densities and, in particular, the large negative spin densities directed away from the oxygen atoms can be understood in terms of usual exchange correlation effects.



Analysis of the multipole moments show that the orbital populations are 0.90(1)e and 0.10(1)e respectively on the copper and oxygen atom. Obviously the system is too complex to analyse by the sophisticated theories we have invoked earlier; but we can clearly see that neutron scattering experiments can clarify exchange processes in discrete binuclear systems and, indeed, in extended ferromagnetic molecular crystals such as phthalocyaninato manganese(II) (Ref. 24).

#### The way ahead

We have demonstrated that the relatively new technique of polarised neutron scattering is capable of giving experimental information on the chemical bond in simple complexes such as  $\text{CrF}_6^{3-}$  and  $\text{CoCl}_4^{2-}$ . The data represent a critical test for theory, only unrestricted Hartree-Fock calculations providing eigenfunctions of sufficient accuracy to match experiment. It is of obvious interest to now begin thinking what form of semi-empirical, if not 'back of envelope', theory can meet the stringent test of experiment. So far as more complex molecules are concerned: under study at present are phthalocyaninato cobalt(II) ( $s = \frac{1}{2}$ ) and phthalocyaninatomanganese(II) ( $s = \frac{3}{2}$ ); at present our view is that, even with fairly extensive experimental data, it will be fairly difficult to provide comprehensive spin densities in as weak a paramagnet as the cobalt(II) complex but this situation could change quite quickly as new higher-flux neutron sources become available.

We can obviously anticipate a growing contribution of these studies to exchange phenomena in finite and infinite arrays and, no doubt, a better understanding between magnetic properties and exchange mechanisms. In a similar way, mixed valence compounds and electron transfer processes and reactions are amenable to much more direct examination. The high selectivity of magnetic scattering also points to studies of very large molecular systems (such as metalloenzymes) in that specific information on the transition metal site may be obtained without recourse to a total structural analysis.

It is salutary, therefore, to recognise the paradox that one of the most powerful probes of the chemical bond in transition metal complexes resides in essentially non-bonding, unpaired electrons. The magnetochemical criterion of stereochemistry has evolved into a comprehensive description of the very subtle features underlying the formation of metal-ligand bonds.

Acknowledgement -- This work was supported by a grant from the Science Research Council, U.K.

## REFERENCES

1. B. Dawson, Proc. Roy. Soc. A298, 264, 379, 395 (1967).
2. R. Mason, Proc. Roy. Soc. A258, 302 (1960).
3. P. Coppens, Measurement of Electron Densities in Solids by X-ray Diffraction, MTP. Inter. Rev. of Science, Phys. Chem. Series, Butterworth, London (1975).
4. R. Mason and J.N. Varghese, J. Organometal. Chem. 181, 159 (1979).
5. P. Coppens. Paper to be submitted at XXI International Conference on Coordination Chemistry, Toulouse, July (1980).
6. B.C. Tofield, Structure and Bonding, Springer-Verlag, Berlin, Vol.21 (1975).
7. F.A. Wedgwood, Proc. Roy. Soc. London, A349, 447 (1976).
8. B.N. Figgis, R. Mason, A.R.P. Smith, J.N. Varghese and G.A. Williams, to be published (1980).
9. W. Marshall and S.W. Lovesy, Theory of Thermal Neutron Scattering, Oxford, Clarendon Press (1971).
10. B.N. Figgis, R. Mason, A.R.P. Smith and G.A. Williams, J. Amer. Chem. Soc. 101, 3673 (1979).
11. B.N. Figgis, P.A. Reynolds and G.A. Williams, J.C.S. Dalton, in press (1980).
12. R.F. Stewart, J. Chem. Phys. 58, 1668 (1973).
13. R.F. Stewart, Acta Cryst. A32, 565 (1976).
14. P.F. Price, Ph.D. Thesis, University of Western Australia (1976).
15. P. Coppens, T.N. Guru Row, P. Leung, E.D. Stevens, P.J. Becker and Y.W. Yang, Acta Cryst. A35, 63 (1978).
16. J.N. Varghese and E.N. Maslen, unpublished results (1975).
17. J.N. Varghese and R. Mason, Proc. Roy. Soc. in press (1980).
18. R. Mason and J.N. Varghese, to be published (1980).
19. R.D. Brown and P.G. Burton, Theoret. Chim. Acta. (Berl.) 18, 309 (1970).
20. A. Tang Kai and S. Larsson, Int. J. Quantum Chem. 13, 375 (1978).
21. R. Mason, A.R.P. Smith, J.N. Varghese, to be published (1980).
22. B.N. Figgis, R. Mason, P.A. Reynolds, A.R.P. Smith, J.N. Varghese and G.A. Williams, J.C.S. Dalton, in press (1980).
23. R. Mason, A.R.P. Smith and J.N. Varghese, to be published (1980).
24. G.A. Williams, B.N. Figgis and R. Mason, to be published (1980).
25. F.A. Cotton and R. Mason, private communication.